Journal of Anatomy

J. Anat. (2010) **217**, pp245–253 doi: 10.1111/j.1469-7580.2010.01265.x

The presence of accessory cusps in chimpanzee lower molars is consistent with a patterning cascade model of development

Matthew M. Skinner* and Philipp Gunz*

Department of Human Evolution, Max Planck Institute for Evolutionary Anthropology, Leipzig, Germany

Abstract

Tooth crown morphology is of primary importance in fossil primate systematics and understanding the developmental basis of its variation facilitates phenotypic analyses of fossil teeth. Lower molars of species in the chimp/human clade (including fossil hominins) possess between four and seven cusps and this variability has been implicated in alpha taxonomy and phylogenetic systematics. What is known about the developmental basis of variation in cusp number – based primarily on experimental studies of rodent molars – suggests that cusps form under a morphodynamic, patterning cascade model involving the iterative formation of enamel knots. In this study we test whether variation in cusp 6 (C6) presence in common chimpanzee and bonobo lower molars (n = 55) is consistent with predictions derived from the patterning cascade model. Using microcomputed tomography we imaged the enamel-dentine junction of lower molars and used geometric morphometrics to examine shape variation in the molar crown correlated with variation in C6 presence (in particular the size and spacing of the dentine horns). Results indicate that C6 presence is consistent with predictions of a patterning cascade model, with larger molars exhibiting a higher frequency of C6 and with the location and size of later-forming cusps correlated with C6 variation. These results demonstrate that a patterning cascade model is appropriate for interpreting cusp variation in *Pan* and have implications for cusp nomenclature and the use of accessory cusp morphology in primate systematics.

Key words accessory cusp; cusp 6; cusp nomenclature; odontogenesis; *Pan*.

Introduction

There is considerable variation in the number of cusps on living and extinct primate molar teeth and this variation is used to identify and define species and infer their phylogenetic relationships. For example, extant hominoid and fossil hominin lower molars tend to have five primary cusps, but between four and seven cusps can be present. Interpreting this variability in cusp number and location is hampered by a limited understanding of the developmental processes controlling cusp development in primates. This leads to disagreements regarding cusp nomenclature, the status of cusps as either primary or accessory, the homology of cusps among different species, and the interpretation of cusp patterning in primate systematics (e.g. Biggerstaff, 1968; Keene, 1994; Skinner et al. 2008).

Studies of developing murine teeth (Jernvall, 2000; Jernvall & Thesleff, 2000; Salazar-Ciudad & Jernvall, 2002; Kangas et al. 2004; Kassai et al. 2005), computational modelling of mammalian tooth development (Salazar-Ciudad & Jernvall, 2002, 2010), and variation in cusp patterning in seals (Jernvall, 2000) suggest that cusp initiation and patterning in tooth germs is an iterative process that repeatedly utilizes the same developmental pathway. It has been demonstrated that cusp spacing in mice is controlled by the nested expression of activator and inhibitor proteins in the dental epithelium and mesenchyme in the developing tooth germ (Jernvall & Thesleff, 2000; Kassai et al. 2005). Additional enamel knots (which result in additional cusps) can form outside the zones of inhibition of previously formed enamel knots. This is a morphodynamic process, meaning that the patterning of cusps on the tooth germ is not predetermined, but rather the size, shape and location of the first-forming cusps influences those same characteristics in later-forming cusps (Salazar-Ciudad & Jernvall, 2002). This process has been called the patterning cascade model of cusp development (Polly,

Correspondence
Matthew M. Skinner and Philipp Gunz, Department of Human Evolution, Max Planck Institute for Evolutionary Anthropology, Leipzig, Germany. E: skinner@eva.mpg.de or gunz@eva.mpg.de

**These authors contributed equally to this paper.*

Accepted for publication *2 June 2010*
Article published online *12 July 2010*

1998; Jernvall, 2000). In this model, small changes early in the development of the tooth germ can result in large differences in the fully formed tooth crown, particularly in the number of cusps.

A number of previous studies support the hypothesis that cusp patterning in human molars is consistent with the patterning cascade model. In a study of monozygotic and dizygotic twins, Townsend et al. (2003, p. 354) found that intercuspal distances were more variable and exhibited greater fluctuating asymmetry than overall crown dimensions. They therefore concluded that the location of tooth cusps is 'determined by a cascade of epigenetic events, rather than being under direct genetic control'. Both Kondo & Townsend (2006) and Harris (2007) found that an accessory cusp present on upper molars, the Carabelli's cusp, was more likely to be present on larger molars due to reduced spatial constraints on secondary enamel knot formation. However, it remains unclear whether it is appropriate to always use a patterning cascade model in interpreting the variation in cusp number and cusp patterning in extant apes and humans (and their fossil relatives).

In this study we use the morphology of fully formed teeth to assess whether processes controlling cusp patterning in chimpanzee molars are consistent with predictions based on the patterning cascade model. Rather than using the outer enamel surface, we study the enamel-dentine junction (EDJ), which is the interface between the enamel cap and the dentine crown, for the following reasons. First, the EDJ preserves a morphological record of the developmental surface upon which cusps form. Specifically, it is a proxy for the basement lamina present in the developing tooth germ, which is located between the internal enamel epithelium and dental papilla. Current developmental models focus on the growth and folding of the internal enamel epithelium, making the EDJ the most appropriate structure of fully formed teeth upon which to test hypotheses of tooth development in apes and humans. The second reason we study the EDJ is that the presence and relative size of cusps (in this case dentine horns) can be examined more accurately at the EDJ than at the enamel surface, which tends to exhibit varying degrees of dental attrition in museum and fossil specimens.

In a patterning cascade model of cusp development, a number of developmental parameters can influence the variable presence of accessory cusps. These parameters include the overall size of the tooth germ, the relative timing of cusp initiation, and the interaction of initiation/inhibitor gene products expressed in the developing germ. With these parameters in mind, predictions can be made regarding the morphology of the EDJ and the variable presence of accessory cusps. For this study, we analyzed the correlation between EDJ shape and the variable presence of cusp 6 (C6). C6 forms on the distal margin of lower molars between the hypoconulid and entoconid (see Keene, 1994 for a comprehensive review of the C6) and is variably present in almost all extant and fossil species within the chimp/human clade. Figure 1a shows a partially worn C6 on the outer enamel surface of a chimpanzee lower molar and its underlying dentine horn at the EDJ. Figure 1b schematically illustrates the hypothesized interaction between developmental parameters of molar growth and the variable presence of a C6. A C6 is unlikely to form when tooth germ size is reduced, when the degree of inhibition is increased, and/or when the hypoconulid and entoconid are forming coincidentally. Conversely, a C6 is likely to form with an increase in tooth germ size, a decrease in the degree of inhibition, and/or when the initiation of the hypoconulid and entoconid is staggered. Similarly, the interaction of these three factors could theoretically lead to the formation of an additional cusp adjacent to the C6. If cusp patterning in chimpanzee molars follows a patterning cascade model, a C6 is predicted to occur more frequently in molars with larger EDJs and/or in molars whose distal dentine horns are relatively small and widely spaced.

Materials and methods

To detect and analyze the dentine horns of both primary cusps and C6s on chimpanzee lower molars we employed high-resolution microcomputed tomography (microCT) to non-destructively image the EDJ. We used microCT to produce surface models of the EDJ of *Pan* lower molars and geometric morphometrics to characterize shape variation between molars with and without a C6. Using multivariate statistical analysis and visualization tools we tested the above predictions regarding EDJ size and shape, the size and position of the primary cusps, and the presence of a C6.

Study sample

The study sample consists of first and second lower molars (n = 55) of *Pan paniscus* and *Pan troglodytes*. The *Pan paniscus* sample (n = 17) is from the Royal Museum for Central Africa collection in Tervuren, Belgium. Part of the *Pan troglodytes* sample (n = 21) is in the collection of the Museum für Naturkunde in Berlin, Germany, and represents primarily the subspecies *Pan troglodytes troglodytes* (n = 12) but includes some specimens of unknown subspecies affiliation (n = 9). The second part of the sample includes *Pan troglodytes verus* specimens (n = 17) from a skeletal collection housed at the Max Planck Institute for Evolutionary Anthropology in Leipzig, Germany, and is derived from deceased individuals collected within the research mandate of the Taï Chimpanzee Project based in the Taï National Park, Republic of Côte d'Ivoire. Taxonomic designation is based on locality information and museum catalogue information associated with each specimen.

MicroCT and EDJ surface reconstruction

Each tooth was microCT scanned using a SKYSCAN 1172 Desktop Scanner (100 kV, 94 μA, 2.0 mm aluminium and copper filter, 0.12 rotation step, 360 degrees of rotation, 2-frame averaging). Pixel dimensions and slice spacing of the resultant images ran-

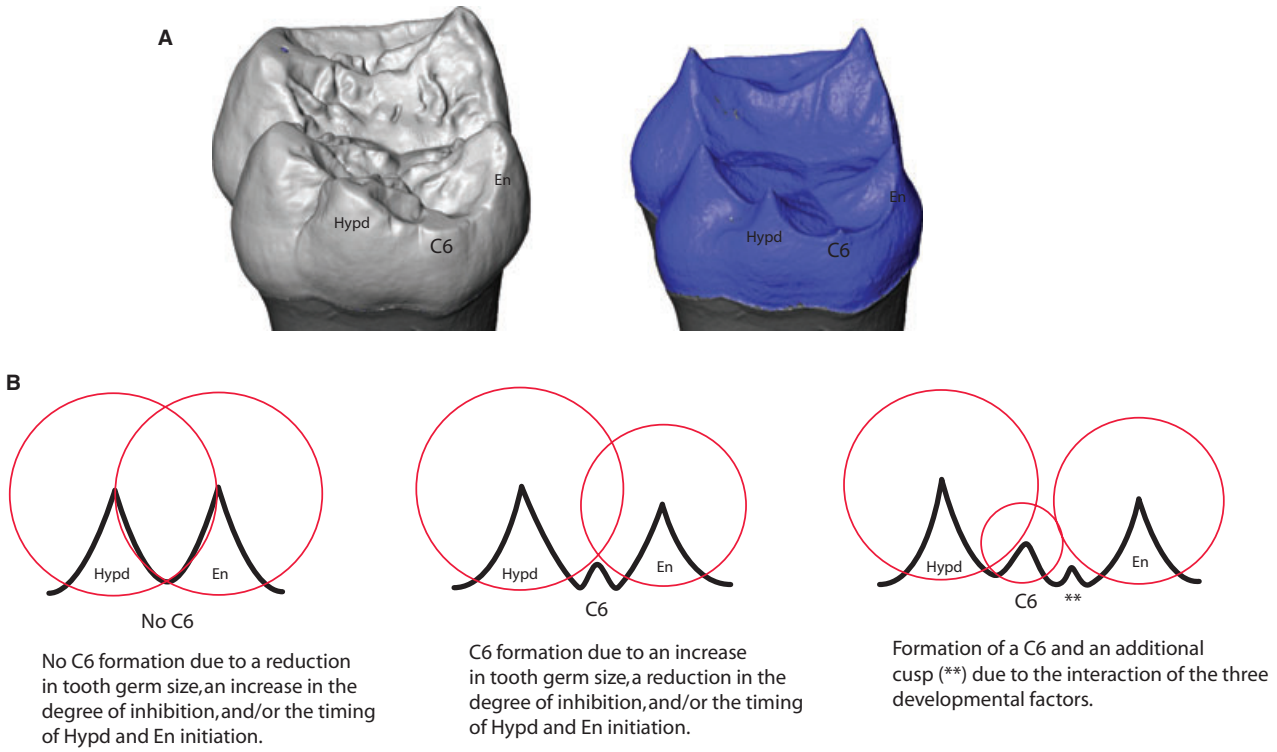

Fig. 1 (A) Digital model of a chimpanzee lower molar showing the presence of a cusp 6 (C6) at the outer enamel surface (left) and EDJ (right). (b) Schematic representation of the hypothetical relationship between the developing dentine horns (black peaks) of the hypoconulid (Hypd) and entoconid (En), the zones of inhibition of secondary enamel knots (red circles) and the variable presence of a C6.

ged between 10 and 20 μm. To facilitate tissue segmentation, the complete image stack for each tooth was filtered (using both a median and a mean-of-least-variance filter; kernel sizes of 3) and enamel and dentine tissues were segmented using Avizo v6.0 (www.vsg3d.com). After segmentation, the EDJ was reconstructed as a triangle-based surface model.

Scoring procedure

Cusp 6 was scored as present if a dentine horn was discernible between the hypoconulid and entoconid dentine horns. Some molars in the sample exhibited a very slight elevation on the marginal ridge in the C6 location. As it was unclear whether such a feature represents a very small and poorly developed C6 dentine horn, or simply an elevation on the marginal ridge, these molars were scored as having a 'suspected' C6. Scoring was conducted independently by each author with 96% scoring consistency (53 of 55 teeth). Scoring was repeated after 3 months by MMS with 93% scoring consistency (51 of 55 teeth).

Geometric morphometric analysis

The EDJ surface models were imported into AMIRA for the collection of two sets of 3D anatomical landmarks (see Fig. 2). The first set (referred to as 'MAIN') included eight landmarks: one on the tip of the dentine horn of each primary cusp, one at the mid-point on the marginal crest connecting the protoconid and metaconid, and one each on the lowest point on the marginal ridges between the protoconid and hypoconid, and the hypoconid and hypoconulid, respectively. The second set (referred to as the 'RIDGE' curve) includes coordinates (50–70) along the tops of the ridges that connect the five dentine horns. This set of points forms a continuous line, beginning at the tip of the protoconid and moving in a lingual direction. In the case of molars with a C6, points were collected on either side of its dentine horn. As this curve was later resampled (see below), it was not initially necessary that the same number of points be placed along the curve for each specimen. Thus, the spacing of points was dictated such that they did not touch adjacent neighbours but were not so far apart as to misrepresent aspects of the curve (as represented in Fig. 2).

Derivation of homologous landmarks

Structures considered homologous are assumed to have a common evolutionary origin (Zelditch et al. 2004), but in geometric morphometrics, the term 'homologous landmark' means that the landmark corresponds to the same location on the same homologous structure in different specimens, species or developmental stages. Unlike the eight MAIN landmarks, the coordinates collected along the RIDGE curve are not initially homologous as they differ between specimens in number and in the location along the curve. The process by which a corresponding set of landmarks and semilandmarks (Bookstein, 1997; Gunz et al. 2005) was generated for each specimen was as follows. First, for the RIDGE landmarks a smooth curve was fitted by starting at an initial point (the tip of the protoconid dentine horn) and moving lingually around the curve. A cubic spline was used so that the curve is forced to pass through each measured coordinate. The eight MAIN homologous landmarks were pro-

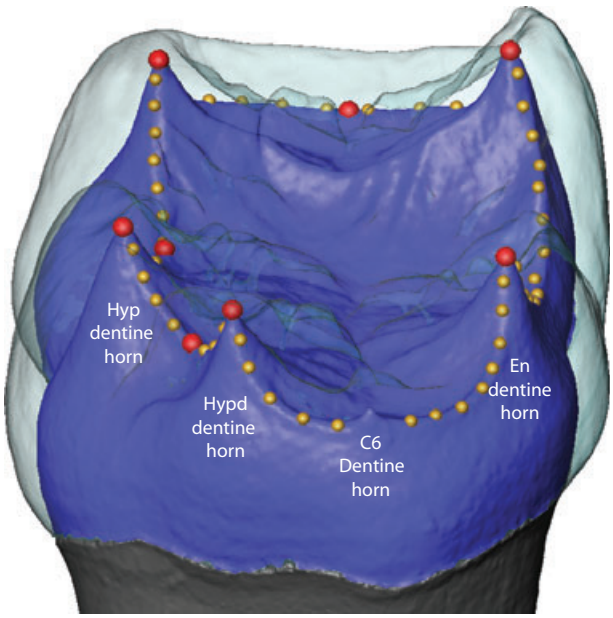

Fig. 2 Distal view of a digital model of a chimpanzee lower molar crown with the enamel cap rendered as transparent to reveal the surface of the EDJ (blue). Landmarks used to capture the relative size and positioning of the dentine horns are shown as spheres (red spheres are MAIN landmarks and yellow spheres are RIDGE curve landmarks). A C6 dentine horn can be seen on the distal margin of the molar crown but is purposefully not included in the RIDGE curve landmark set. See text for details. Hyp, hypoconid; Hypd, hypoconulid; En, entoconid.

jected onto the RIDGE curve, dividing it into eight sections. For each section, a large sample of very closely spaced coordinates was computed along the curve, and the distances between adjacent coordinates were calculated and summed together to approximate the length along the curve segments between the MAIN landmarks. Each length was divided by a given number, based on an estimate of the relative contribution of each section to the RIDGE curve across the molars in the study sample, and the coordinate location at each equally spaced distance was recorded (see Fig. 1 in Skinner et al. 2009a,b). Thus, at this stage, all specimens had the same total number of landmarks (i.e. the homologous, fixed, landmarks on the tips of the dentine horns, plus equal numbers of semilandmarks).

We used the algorithm described by Gunz et al. (2005, 2009), which allows semilandmarks to slide along tangents to the curve. These tangents were approximated for each semilandmark as the vector between the two neighbouring points. Semilandmarks were iteratively allowed to slide along their respective curves to minimize the bending energy of the thin-plate spline interpolation function computed between each specimen and the Procrustes average for the sample. After the application of the sliding algorithm, the eight fixed landmarks and the 52 semilandmarks for the RIDGE curve were considered homologous among each of the study specimens. Each set of landmarks and semilandmarks was converted to shape coordinates by generalized least squares Procrustes superimposition (Gower, 1975; Rohlf & Slice, 1990). This removed information about location and orientation from the raw coordinates and standardized each specimen to unit centroid size; a size-measure computed as the square root of the sum of squared Euclidean distances from each (semi)landmark to the specimen's centroid (Dryden & Mardia, 1998). All data processing was done in MATHEMATICA v6.0 (www. wolfram.com) using a software routine written by P. Gunz.

Visualization of EDJ shape variation

To visualize the shape variation associated with the presence of a C6, we employed a method which allows a 3D triangulated EDJ surface reconstruction to be deformed to match the mean configuration of each group (Gunz et al. 2005; Gunz & Harvati, 2007). First, several thousand points were measured on the EDJ of one specimen and converted to a triangulated surface using the *wrap* module in GEOMAGIC STUDIO 10 (http://www.geomagic.com). This module creates a surface model consisting of triangles formed between adjacent points. We then warped the vertices of this surface into Procrustes space using the thin-plate spline interpolation function between the landmark and semilandmark configuration of this specimen and the Procrustes average configuration of the whole sample. Finally, we computed a thin-plate spline between this mean configuration and each target shape (e.g. the mean configuration of molars with, and without, a C6) to produce a surface model of the appropriate mean shape. Additionally, we exaggerated the deformation along the vector separating the two group means by a factor of two to better visualize those areas of EDJ shape change between molars with and without a C6.

Statistical analysis

A *t*-test was used to test for significant differences in centroid size between first and second molars. As this test was non-significant ($P = 0.15$) first and second molars were combined to test for significant differences in centroid size between molars with and without a C6. All statistical analyses were conducted in SPSS 15 (http://www.spss.com).

Results

The range of variation in C6 expression at the EDJ surface is illustrated in Fig. 3 and can divided into three types. The first type, represented by 21 molars in the sample, exhibits no evidence of a C6 dentine horn on the marginal ridge between the hypoconulid and entoconid (Fig. 3A). Thirteen molars exhibit the second type, which is a slight raised elevation on the marginal ridge between the hypoconulid and entoconid that lacks the typical morphology of a dentine horn with a conical point (Fig. 3B). For the purpose of analysis these specimens are treated as having a 'suspected' C6. The third type is a clearly discernible C6 dentine horn, which is present in 21 molars of the study sample (Fig. 3C). Three molars in the sample exhibit two dentine horns between the hypoconulid and entoconid (Fig. 3D). How these latter three morphological variants fit into the patterning cascade model is discussed below, but for the purpose of analyzing EDJ shape variation correlated with C6 presence/absence they are treated as having the C6 present.

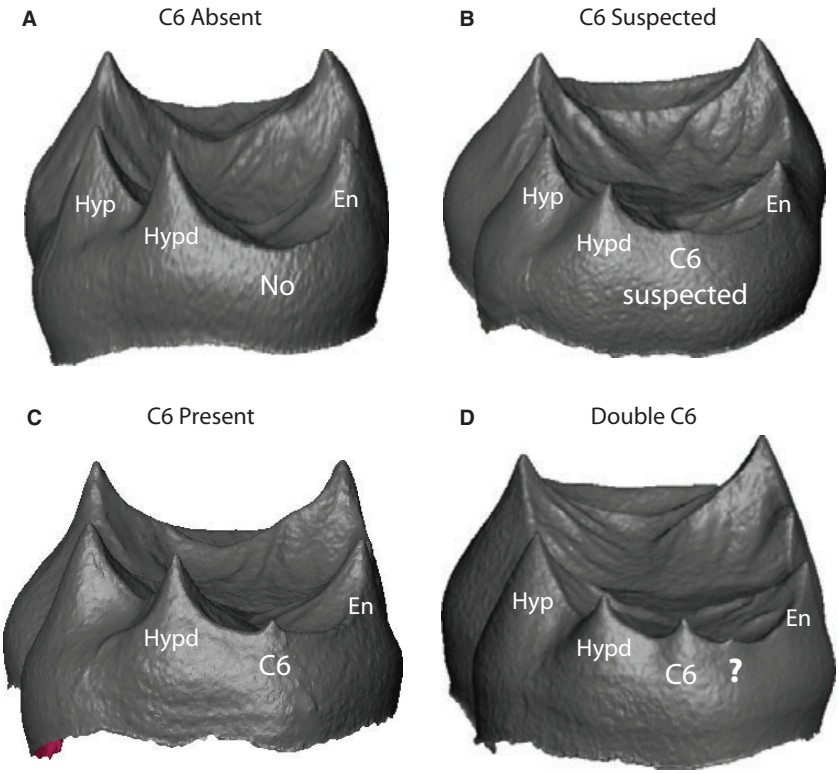

Fig. 3 Digital surface models of the EDJ of four molars illustrating variation in C6 manifestation. (A) No evidence of a C6 dentine horn; (B) a slight elevation is present on the marginal ridge between the hypoconulid (Hypd) and entoconid (En) representing a suspected C6; (C) an unambiguous C6 dentine horn; and (D) the presence of an additional dentine horn mesial to the C6 dentine horn which demonstrates the developmental origin of a so-called 'double C6' at the enamel surface.

The first model prediction is that larger tooth germs will be more likely to possess a C6 based on the rationale that the area of secondary enamel knot inhibition and/or timing of cusp initiation are held constant and therefore a larger tooth germ will have greater potential to form an accessory cusp. Using centroid size as a proxy for overall tooth germ size, the prediction is supported, such that molars possessing a C6 are significantly larger on average than molars lacking a C6 [*t*-test (t) = −2.782; $P = 0.008$]. Table 1 shows the distribution of present, suspected and absent C6s among the study taxa. The difference in these proportions of C6 presence between *Pan paniscus* and *Pan troglodytes* samples is significant (Pearson's $\chi = 7.624$; $P = 0.02$). Given that on average *Pan troglodytes* molars are significantly larger than *Pan paniscus* molars [*t*-test (*t*) = −2.437; $P = 0.018$] the proportional representation of C6 between these taxa is also consistent with the first prediction.

The second prediction is that the relative size and location of the distal dentine horns (i.e. hypoconid, hypoconulid and entoconid) will be correlated with the presence of a C6. This prediction is based on the idea that if tooth germ size is held constant and/or there is an increase in the spacing between primary dentine horns, there will be space for accessory cusps to be initiated. To test this prediction we conducted a geometric morphometric analysis of the relative size, shape and spacing of the dentine horns of the five primary cusps. A principal component analysis of shape variation in the total *Pan* sample is presented in Fig. 4A. The degree of clustering between each group suggests that although C6 variation does account for some degree of overall shape variation, there is considerable overlap in overall EDJ shape among the molars in the study sample. Figure 5A illustrates the difference in average shape between molars possessing a C6 and those lacking a C6, as

Table 1 Cusp 6 presence in the study sample.*

Taxon	Cusp 6 present	Cusp 6 suspected	Cusp 6 absent
Pan paniscus	3 (18%)	3 (18%)	11 (64%)
Pan troglodytes	18 (48%)	10 (26%)	10 (26%)
Pan troglodytes verus	11 (64%)	5 (30%)	1 (6%)
Pan troglodytes troglodytes	3 (25%)	3 (25%)	6 (50%)
Pan troglodytes ssp.	4 (na)	2 (na)	3 (na)
All *Pan*	21 (38%)	13 (24%)	21 (38%)

*Percentages are rounded to nearest percent and not applicable (na) for *Pan troglodytes* of unknown subspecies.

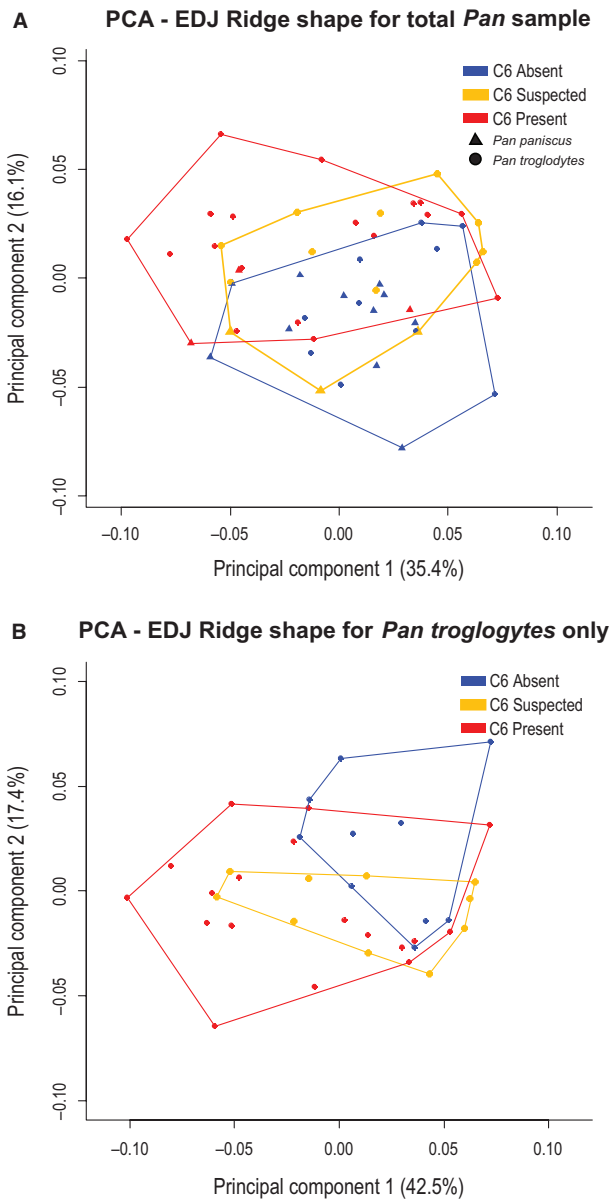

Fig. 4 Plots of the first and second principal components of an analysis of EDJ ridge shape variation between molars with variable expression of a C6. (A) Analysis of all molars in the sample; (B) analysis of the *Pan troglodytes* sample only. Colors correspond to the presence (red), suspected presence (yellow), and absence (blue) of a C6. (A) *Pan paniscus* specimens symbolized by triangles and *Pan troglodytes* by circles.

well as exaggerated versions of each to highlight those aspects of dentine horn size and spacing associated with C6 variation. Specifically, molars with a C6 tend to have shorter and more widely spaced distal dentine horns compared to the opposite trend in molars lacking a C6. This association between dentine horn size and spacing and the presence of a C6 is consistent with the patterning cascade model.

To confirm that the pattern seen in the total *Pan* sample was not driven by the variation in C6 presence among the different species (noted above), we conducted the same analysis but limited to the *Pan troglodytes* sample. Figure 4B presents a PCA of this sample and Fig. 5B illustrates the mean EDJ shape of molars with and without a C6. The pattern of shape variation in the *Pan troglodytes* sample matches that found in the total *Pan* sample, such that molars with a C6 are slightly shorter and have more widely spaced dentine horns than molars lacking a C6. Thus, the predicted relationship between dentine horn size and spacing and C6 presence holds at both the genus and species level.

We also assessed whether the above results could be explained solely by variation in tooth size. Because larger teeth will also tend to have wider dentine horn spacing, the relationship between C6 presence and dentine horn spacing might be a spurious correlation with overall tooth size. Figure 6 plots the centroid sizes (as a measure of overall tooth size) for *Pan troglodytes* teeth without a C6 (red), with a suspected C6 (blue), and with a C6 present (green). As was noted previously, molars with a C6 (or suspected C6) are on average larger than the teeth without a C6; however, the lower size ranges of each group overlap. As imaged in Fig. 6 the smallest molars in each group differ in shape as predicted by the model; with molars possessing or having a suspected C6 exhibiting an entoconid and hypoconulid dentine horn that are more widely spaced than the similarly small-sized molar without a C6. Thus, in molars of the same size, C6 presence is correlated with predicted differences in dentine horn spacing.

Discussion

Overall, the results of this analysis of *Pan* EDJ morphology and the presence of accessory cusps are consistent with a patterning cascade model that is functioning as a morphodynamic process (*sensu* Salazar-Ciudad & Jernvall, 2002, 2010). As predicted, larger *Pan* molars have a higher frequency of C6, as do molars whose later-forming, distal dentine horns are relatively short and widely spaced. The cases of a 'suspected' C6 could represent a small, poorly developed C6 that, while initiated due to available space between adjacent cusps, did not progress substantially in growth prior to the mineralizing fronts of dentine and enamel that ended the cell division in the internal enamel epithelium.

A number of molars in the *Pan troglodytes* sample possessed not only a C6 dentine horn but also an associated dentine horn lingually (i.e. the 'double' C6 in Fig. 3). In the dental literature describing cusp morphology one can find terms (or illustrations) indicative of 'double' or 'split' cusps including the C6 (Wood & Abbott, 1983; Aiello & Dean, 1990; Keene, 1994). The morphological patterning of dentine horns identified in this study, interpreted within current developmental models of cusp patterning, suggests that such terms may be invalid and misrepresent the

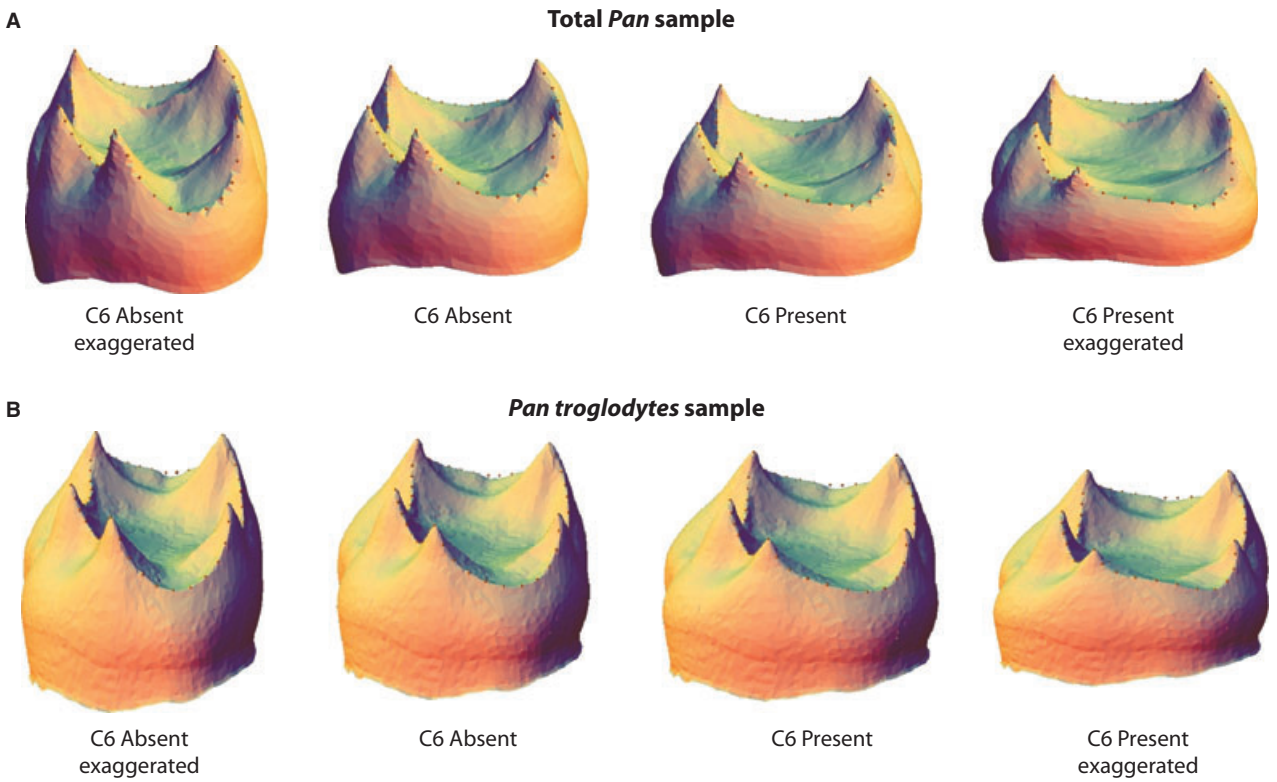

Fig. 5 Digital surface models of the EDJ illustrating average shape differences between molars with and without a C6. To highlight the relationship between dentine horn size and spacing and the variable presence of a C6, the models to the left and right represent 'exaggerated' models. In analyses of the total *Pan* sample (A) and the *Pan troglodytes* sample (B) the presence of a C6 is associated with relatively short and widely spaced distal dentine horns. While there is considerable overlap in overall shape within each molar sample (see Fig. 4), the difference in average shape between molars with and without a C6 is consistent with the predictions of a cascade pattern of cusp development in chimpanzees at both a genus and a species level.

developmental processes underlying cusp variation. Just as a C6 should not be considered a doubled or a split hypoconulid (C5), a cusp adjacent to a C6 should not be considered a doubled or split form of a C6. This extra cusp, like the C6, is the result of the same iterative developmental process underlying the primary cusps. Researchers will need to decide how they will interpret the significance of variation in cusp number and patterning within and between taxa with regard to taxonomic and phylogenetic questions. In particular, scoring systems for accessory cusp variation should be consistent with the results of studies such as this one that support an iterative developmental process of cusp formation rather than a presumption that, for example, a molar exhibits evidence for 'a double C6' in the same way as one might speak of an allele for a particular genetic trait. As was shown by Kondo & Townsend (2006) and Harris (2007) for the Carabelli's trait, we have shown that the occurrence of C6 in the genus *Pan* is not an independent trait, in the cladistic sense, as the expression of this feature is associated with overall tooth size and the morphology of adjacent cusps.

The results of this study have implications for the description of accessory cusps and the interpretation of their variation within and among primate taxa. First, this and a previous study (Skinner et al. 2008) highlight the importance of examining the EDJ to properly identify the presence of accessory cusps and interpret their morphology. It is apparent that accessory cusp development and variability is complex and this has implications for assumptions of homology in cusp patterning between different primate taxa. For example, the C6 dentine horn in chimpanzees is strongly associated with the hypoconulid rather than the entoconid, but this is not consistent among extant and fossil apes and hominins (Skinner et al. 2008). Guatelli-Steinberg & Irish (2005) noted that in recognition of the patterning cascade model, the homology of C6 between *Australopithecus afarensis* and *Paranthropus* (both African fossil hominins) requires further evaluation. Furthermore, Skinner et al. (2009b) suggested that the interaction between dentine horn spacing and crown size could explain the consistent difference in protostylid expression between *Australopithecus africanus* and *Paranthropus robustus*. If accessory cusps form as the result of different developmental patterns, this would complicate the identification of a taxonomic or phylogenetic signal in their variation. The developmental plasticity of mammalian teeth

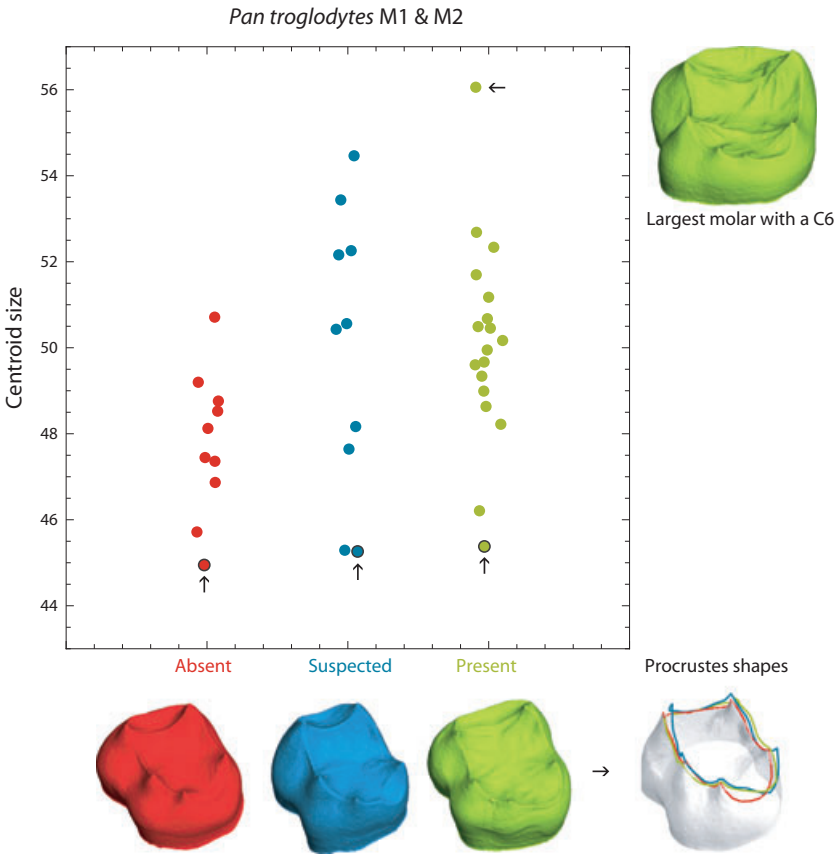

Fig. 6 Centroid size of *Pan troglodytes* molars with no C6 (red), with a suspected C6 (blue) and with a C6 present (green). Molars without a C6 are on average smaller than those with a suspected C6 or a C6 present, but the lower size ranges overlap. The dentine crowns of the smallest molars of each group (arrows) as well as the biggest molar are plotted to scale to show that equally small molars exhibit dentine horn spacing and C6 expression that is consistent with predictions of the patterning cascade model. The Procrustes shape coordinates of the three smallest teeth from each group are superimposed in the lower right corner to highlight the dentine ridge shape differences [for clarity a white surface model is plotted only for the smallest tooth without C6 (red ridge curve); for the other two groups only the ridge curve is plotted].

allows more than one option for the evolution of new cusps, suggesting caution in the assumption of homology between different taxa (Polly, 1998; Jernvall & Salazar-Ciudad, 2007).

There is a strong association between dentine horns and crests at the EDJ and this includes accessory cusps forming along the marginal ridge crests that form between the dentine horns of the primary cusps. We speculate that there exists a developmental constraint in the growing tooth germ that limits where crests and cusps can form. In the Y-5 pattern of the Hominoidea this manifests itself in lower molars as a ring around the margin of the tooth germ corresponding to the distal portion of the trigonid and the whole talonid. It is on this ring that dentine horns for the primary cusps, C6 and cusp 7 form. If additional dentine horns form on the EDJ (for example, beside the C6 or, in the case of anterior marginal ridge tubercles, on upper molars) these also form on this ring. From our observations of hundreds of hominoid teeth it is very rare, for example, for dentine horns of accessory cusps to appear within the occlusal basin. One of the few examples can be seen in the *Gorilla* molar in Skinner et al. (2008; Fig. 3) in which an accessory cusp appears between the hypoconulid and entoconid but not on the distal marginal ridge (although importantly, it is directly associated with a crest). This apparent association between crests and cusps may be related to a highly conserved pattern of expression of inhibitory proteins such as ectodin, which has been implicated in cusp patterning in mice (Kassai et al. 2005).

In this study we have demonstrated that accessory cusp patterning in chimpanzee lower molars is consistent with a morphodynamic, patterning cascade model of cusp development. This finding is consistent with previous studies of other mammalian taxa and supports the hypothesis that this mode of cusp patterning is highly conserved within mammals. It also highlights the importance of understanding the developmental processes underlying tooth crown morphology to incorporate morphological variation among living and extinct taxa into taxonomic and phylogenetic research.

Acknowledgements

This research was supported by Jean-Jacques Hublin, the Department of Human Evolution at the Max Planck Institute for Evolutionary Anthropology, and the Max Planck Society. For access to specimens in their care we thank Emmanuel Gilissen and Wim Wendelen (Royal Museum for Central Africa), and Frieder Mayer, Robert Asher, Hendrik Turni, and Irene Mann (Museum für Naturkunde). We also thank Christophe Boesch for access to the Tai chimpanzee skeletal collection housed at the MPI-EVA. For technical assistance we thank Heiko Temming, Andreas Winzer, and Uta Schwartz. This manuscript was improved

through discussions with Jukka Jernvall, Tracy Kivell and Kornelius Kupczik. We thank Dan Lieberman and two anonymous referees for their comments and constructive criticism that helped improve the manuscript.

Author contributions

M.M.S. and P.G. contributed equally to research design, data acquisition, data analysis and manuscript preparation.

References

Aiello LC, Dean C (1990) *An Introduction to Human Evolutionary Anatomy*. London: Academic Press.

Biggerstaff RH (1968) On the groove configuration of mandibular molars: the unreliability of the '*Dryopithecus* pattern' and a new method for classifying mandibular molars. *Am J Phys Anthropol* **29**, 441–444.

Bookstein FL (1997) Landmark methods for forms without landmarks: morphometrics of group differences in outline shape. *Med Image Anal* **1**, 225–243.

Dryden I, Mardia KV (1998) *Statistical Shape Analysis*. New York: John Wiley & Sons.

Gower JC (1975) Generalized Procrustes analysis. *Psychometrika* **40**, 33–51.

Guatelli-Steinberg D, Irish J (2005) Brief communication: early hominin variability in first molar dental trait frequencies. *Am J Phys Anthropol* **128**, 477–484.

Gunz P, Harvati K (2007) The Neanderthal 'chignon': variation, integration, and homology. *J Hum Evol* **52**, 262–274.

Gunz P, Mitteroecker P, Bookstein FL (2005) Semilandmarks in three dimensions. In: *Modern Morphometrics in Physical Anthropology* (ed. Slice DE), pp. 73–98, New York: Kluwer Academic/Plenum Publishers.

Gunz P, Mitteroecker P, Neubauer S, Weber GW, Bookstein FL (2009) Principles for the virtual reconstruction of hominin crania. *J Hum Evol* **57**, 48–62.

Harris EF (2007) Carabelli's trait and tooth size of human maxillary first molars. *Am J Phys Anthropol* **132**, 238–246.

Jernvall J (2000) Linking development with generation of novelty in mammalian teeth. *Proc Natl Acad Sci U S A* **97**, 2641–2645.

Jernvall J, Salazar-Ciudad I (2007) The economy of tinkering mammalian teeth. *Novartis Found Symp* **284**, 207–216. discussion 216–224

Jernvall J, Thesleff I (2000) Reiterative signaling and patterning during mammalian tooth morphogenesis. *Mech Dev* **92**, 19–29.

Kangas AT, Evans AR, Thesleff I, et al. (2004) Nonindependence of mammalian dental characters. *Nature* **432**, 211–214.

Kassai Y, Munne P, Hotta Y, et al. (2005) Regulation of mammalian tooth cusp patterning by ectodin. *Science* **309**, 2067–2070.

Keene HJ (1994) On the classification of C6 (tuberculum sextum) of the mandibular molars. *Hum Evol* **9**, 231–247.

Kondo S, Townsend GC (2006) Associations between Carabelli trait and cusp areas in human permanent maxillary first molars. *Am J Phys Anthropol* **129**, 196–203.

Polly PD (1998) Variability, selection, and constraints: development and evolution in viverravid (Carnivora, Mammalia) molar morphology. *Paleobiology* **24**, 409–429.

Rohlf FJ, Slice D (1990) Extensions of the Procrustes method for the optimal superimposition of landmarks. *Syst Zool* **39**, 40–59.

Salazar-Ciudad I, Jernvall J (2002) A gene network model accounting for development and evolution of mammalian teeth. *Proc Natl Acad Sci U S A* **99**, 8116–8120.

Salazar-Ciudad I, Jernvall J (2010) A computational model of teeth and the developmental origins of morphological variation. *Nature* **464**, 583–586.

Skinner MM, Wood BA, Boesch C, et al. (2008) Dental trait expression at the enamel–dentine junction of lower molars in extant and fossil hominoids. *J Hum Evol* **54**, 173–186.

Skinner MM, Gunz P, Wood BA, et al. (2009a) Discrimination of extant *Pan* species and subspecies using the enamel-dentine junction morphology of lower molars. *Am J Phys Anthropol* **140**, 234–243.

Skinner MM, Wood BA, Hublin J-J (2009b) Protostylid expression at the enamel-dentine junction and enamel surface of mandibular molars of *Paranthropus robustus* and *Australopithecus africanus*. *J Hum Evol* **56**, 76–85.

Townsend G, Richards L, Hughes T (2003) Molar intercuspal dimensions: genetic input to phenotypic variation. *J Dent Res* **82**, 350–355.

Wood BA, Abbott SA (1983) Analysis of the dental morphology of Plio-Pleistocene hominids I. Mandibular molars: crown area measurements and morphological traits. *J Anat* **136**, 197–219.

Zelditch ML, Swiderski DL, Sheets HD, et al. (2004) *Geometric Morphometrics for Biologists*. New York: Elsevier Academic Press.